International Journal of Wildland Fire 2018, **27**, 595–608
doi:10.1071/WF17122_AC

Supplementary material

Estimating post-fire debris-flow hazards prior to wildfire using a statistical analysis of historical distributions of fire severity from remote sensing data

Dennis M. Staley[A,D], *Anne C. Tillery*[B], *Jason W. Kean*[A], *Luke A. McGuire*[C], *Hannah E. Pauling*[A], *Francis K. Rengers*[A] *and Joel B. Smith*[A]

[A]U.S. Geological Survey, Landslide Hazards Program, Golden, CO 80422, USA.

[B]U.S. Geological Survey, New Mexico Water Science Center, Albuquerque, NM 87113, USA.

[C]University of Arizona, Department of Geosciences, Tucson, AZ 85721, USA.

[D]Corresponding author. Email: dstaley@usgs.gov

Table S1. Comparison of simulated and observed burn severity classes for the 8 test locations. Obs = observed soil burn severity, Sim = simulated soil burn severity, L = low burn severity, H/M = high or moderate soil burn severity.

Fire	Obs = L, Sim = L (%)	Obs = L, Sim = H/M (%)	Obs = H/M, Sim = L (%)	Obs = H/M, Sim = H/M (%)	% Correct	% Incorrect
-	-	-	-	-	-	-
Blue Cut (2016)	**18.3%**	13.0%	23.3%	**45.5%**	**63.8%**	36.2%
First Creek (2015)	**18.2%**	17.0%	28.9%	**35.9%**	**54.1%**	45.9%
Gap (2016)	**31.4%**	56.2%	3.4%	**9.0%**	**40.4%**	59.6%
Hayden Pass (2016)	**0.0%**	0.0%	17.6%	**82.4%**	**82.4%**	17.6%
Junkins (2016)	**2.4%**	3.2%	32.8%	**61.5%**	**64.0%**	36.0%
Pony (2016)	**3.2%**	2.5%	61.6%	**32.7%**	**35.9%**	64.1%
San Gabriel Complex (2016)	**0.0%**	0.0%	19.8%	**80.2%**	**80.2%**	19.8%
Wolverine (2015)	**3.3%**	3.8%	21.0%	**71.9%**	**75.2%**	24.8%
Totals	**11.7%**	15.7%	19.7%	**52.9%**	**64.6%**	35.4%

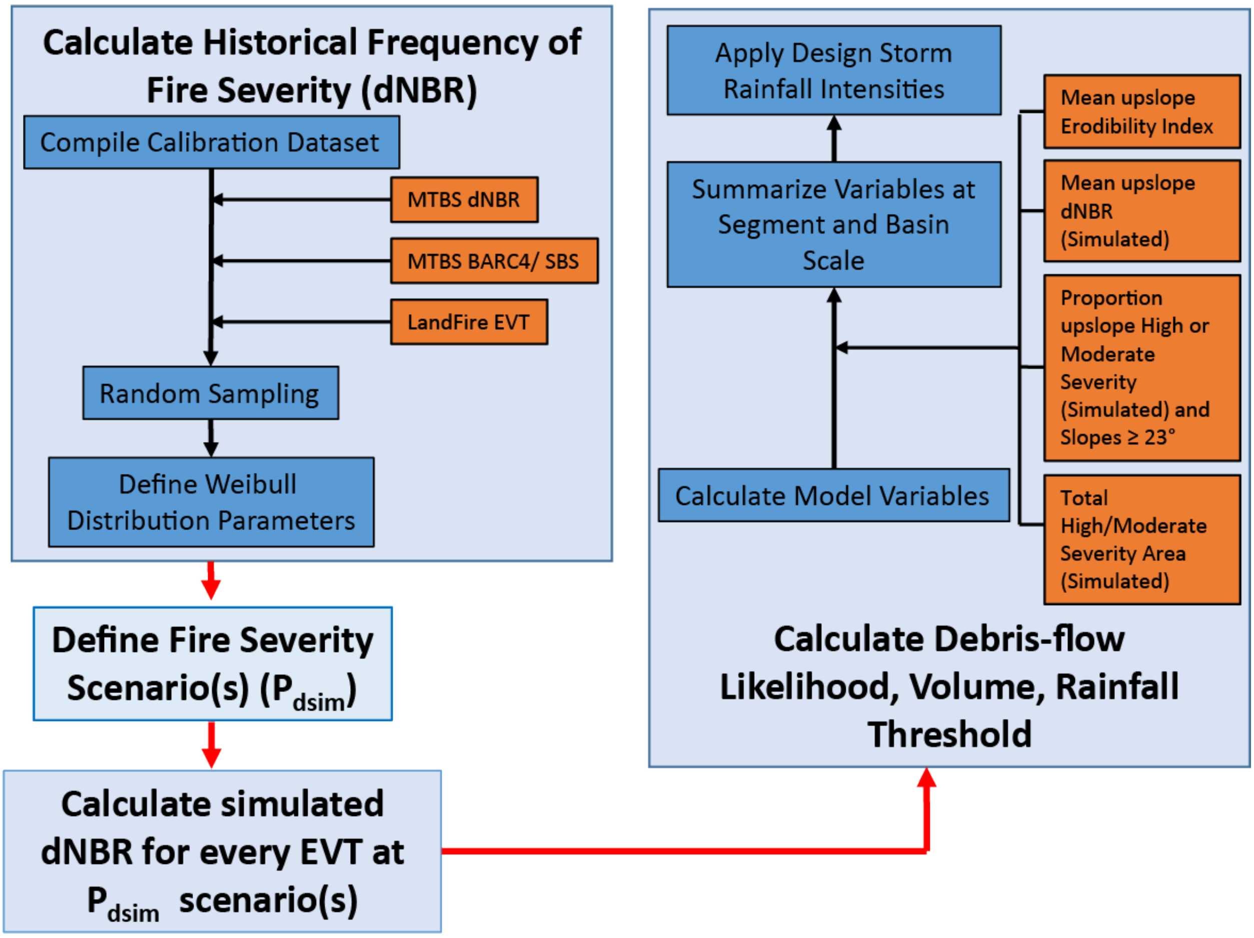

Fig. S1. Processing steps for defining the statistical distribution of fire severity for each Existing Vegetation Type (EVT) and estimating potential debris-flow hazards, including likelihood, volume, and rainfall intensity-duration threshold. dNBR = differenced normalized burn ratio, BARC4 = burned area reflectance classification (4 classes).

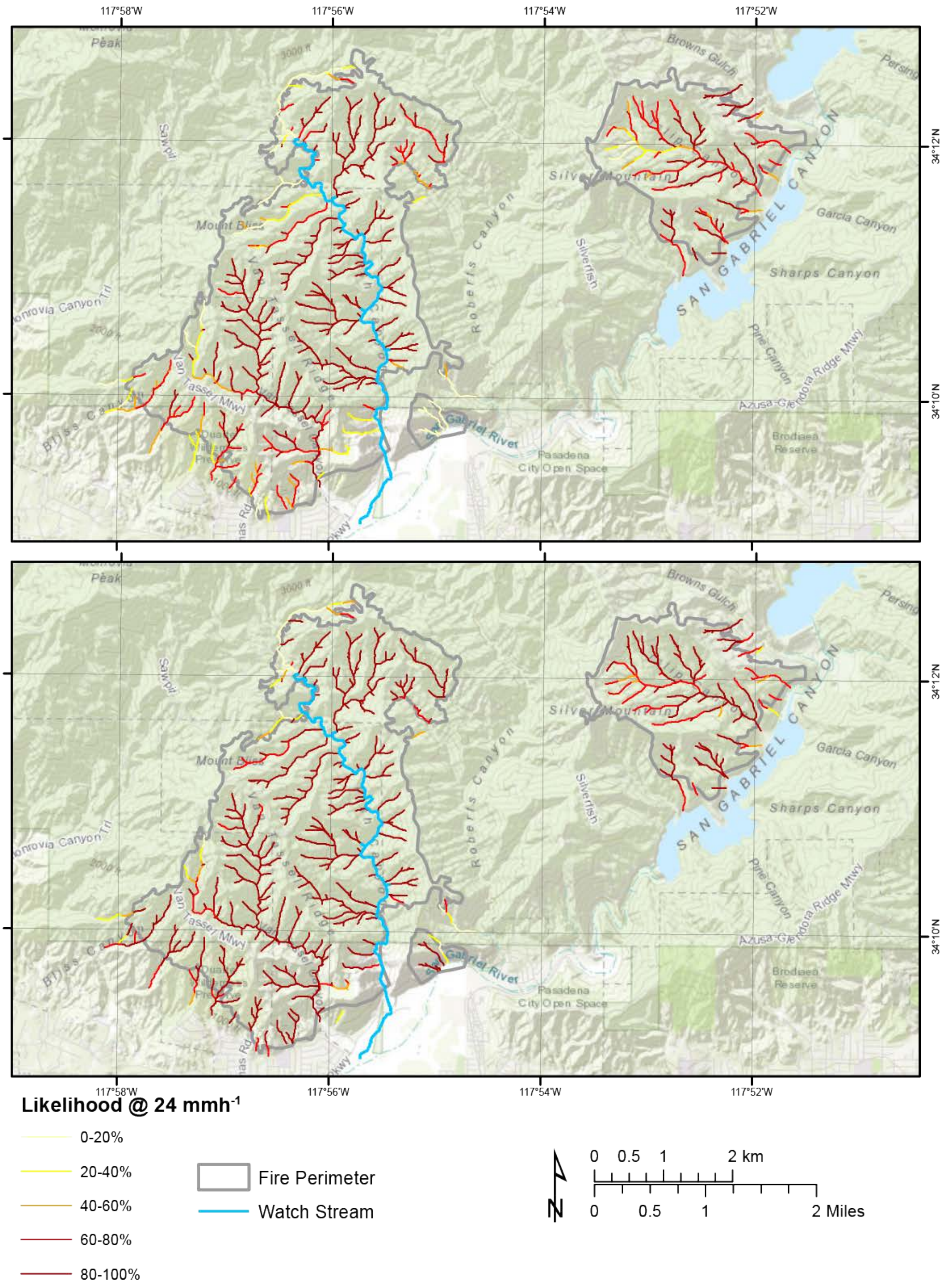

Fig. S2. Comparison of estimated likelihood for a storm with a peak 15-minute rainfall intensity of 24 mmh^{-1} between model runs using observed fire severity data (A), and simulated fire severity data (B) at $P_{dsim} = 0.95$.

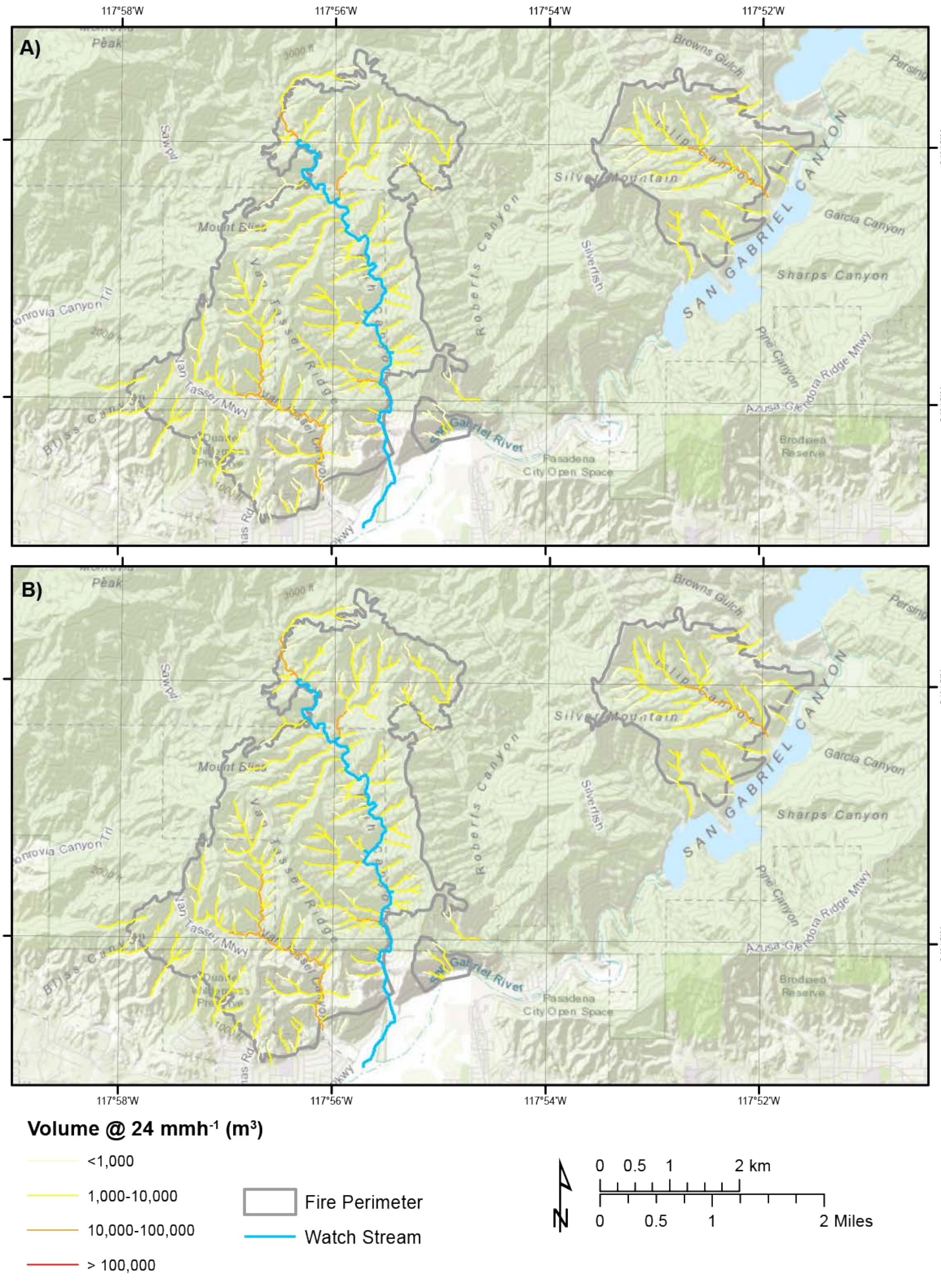

Fig. S3. Comparison of estimated volume (in cubic meters, m^3) for a storm with a peak 15-minute rainfall intensity of 24 mmh^{-1} between model runs using observed fire severity data (A), and simulated fire severity data (B) at P_{dsim} = 0.95.

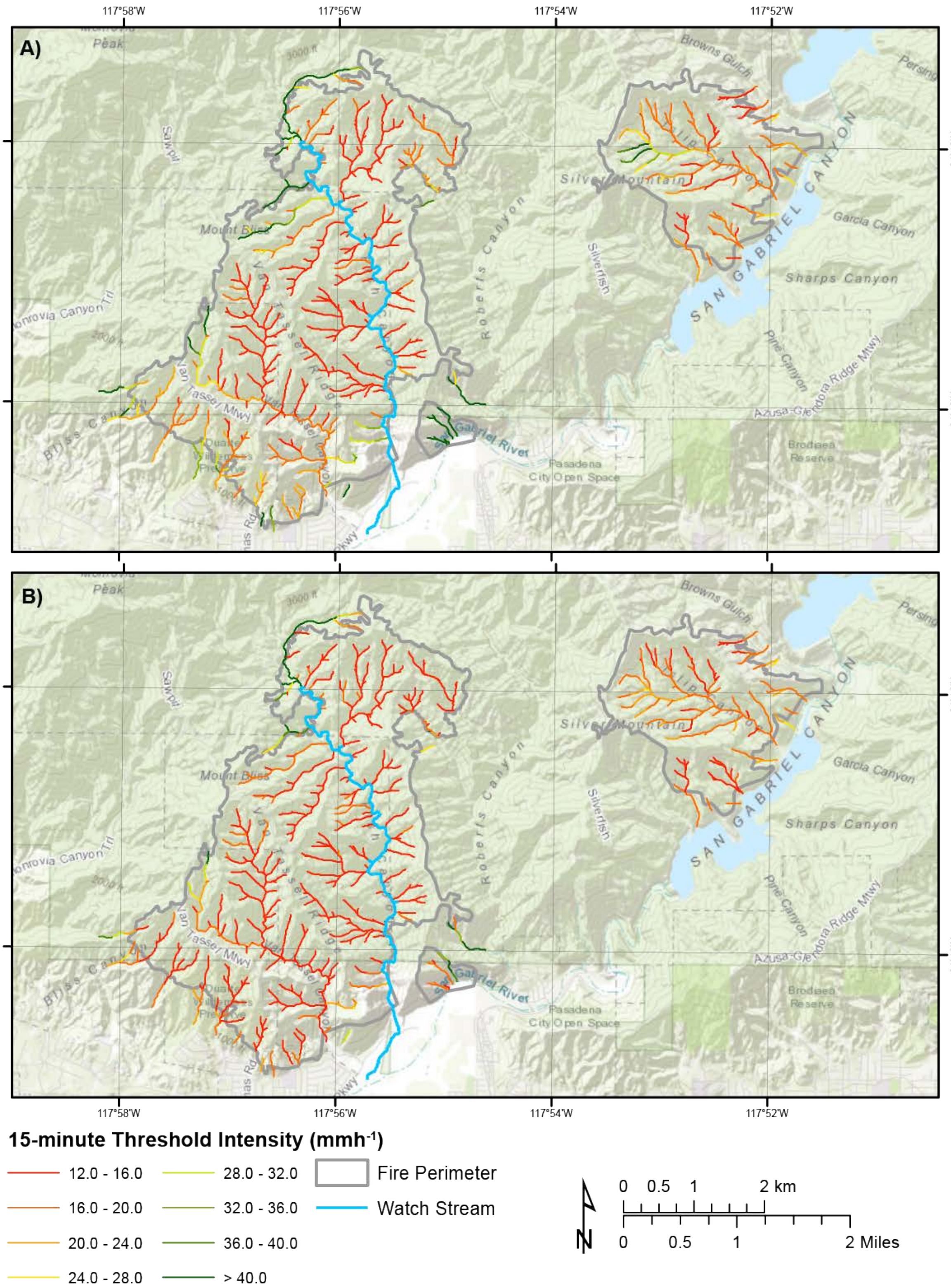

Fig. S4. Comparison of estimated 15-minute rainfall intensity duration threshold, in mmh^{-1}, between model runs using observed fire severity data (A), and simulated fire severity data (B) at $P_{dsim} = 0.95$.

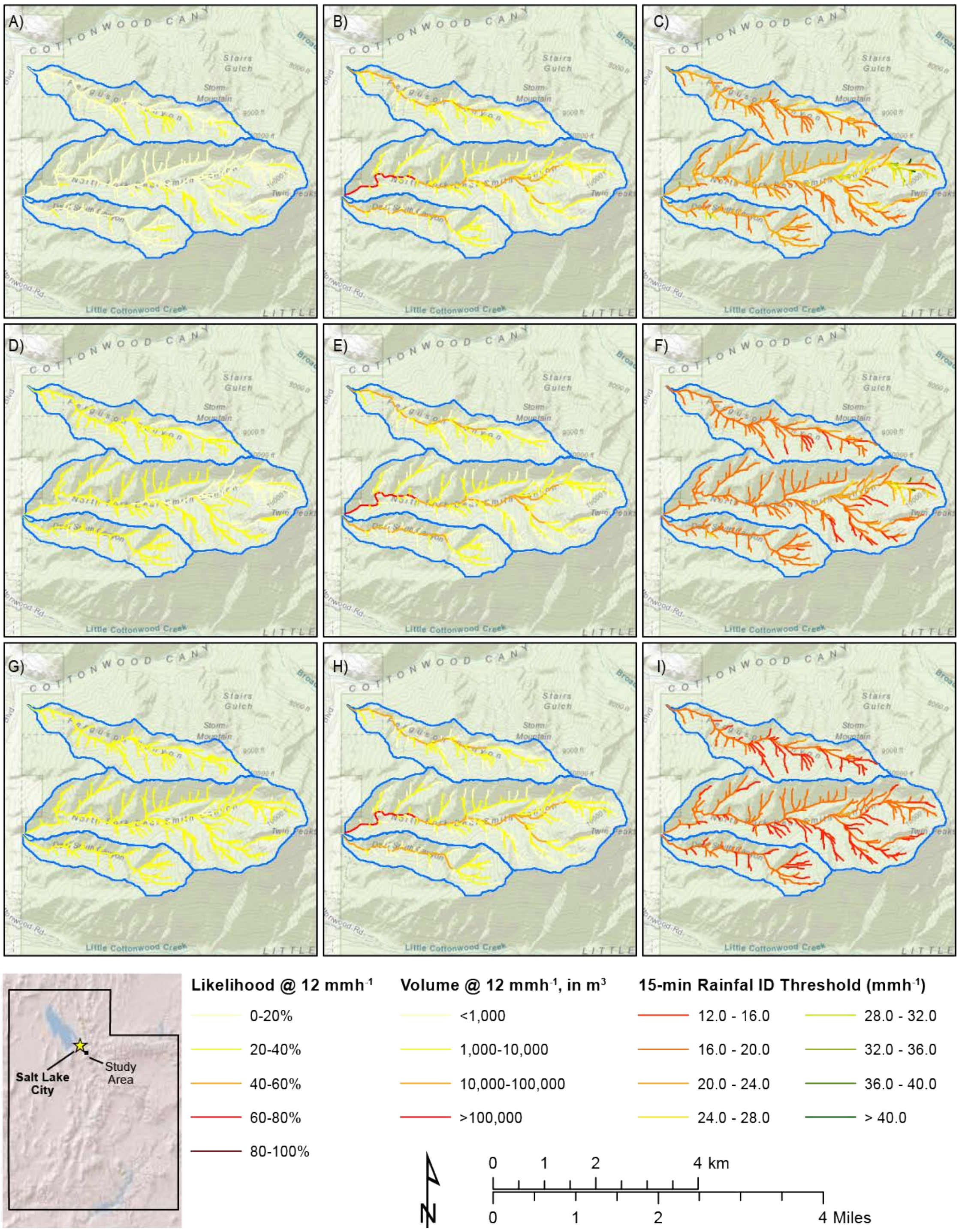

Fig. S5. Simulation results for three canyon above suburban Salt Lake City at three fire severity scenarios: P_{dsim} = 0.5 (A, B, and C), P_{dsim} = 0.75 (D, E, and F), and P_{dsim} = 0.9 (G, H, and I). The three canyons from north to south, are Ferguson Canyon, North Fork Deaf Smith Canyon, and Deaf Smith Canyon. Simulated likelihood (H_L) for a storm with a peak 15-minute intensity of 12 mmh^{-1} (A, D, and G), simulated volume (H_V), in m^3, for a storm with a peak 15-minute intensity of 12 mmh^{-1} (B, E, and H), and simulated 15-minute rainfall intensity-duration threshold (H_{T15}), in mmh^{-1} (C, F, and I).

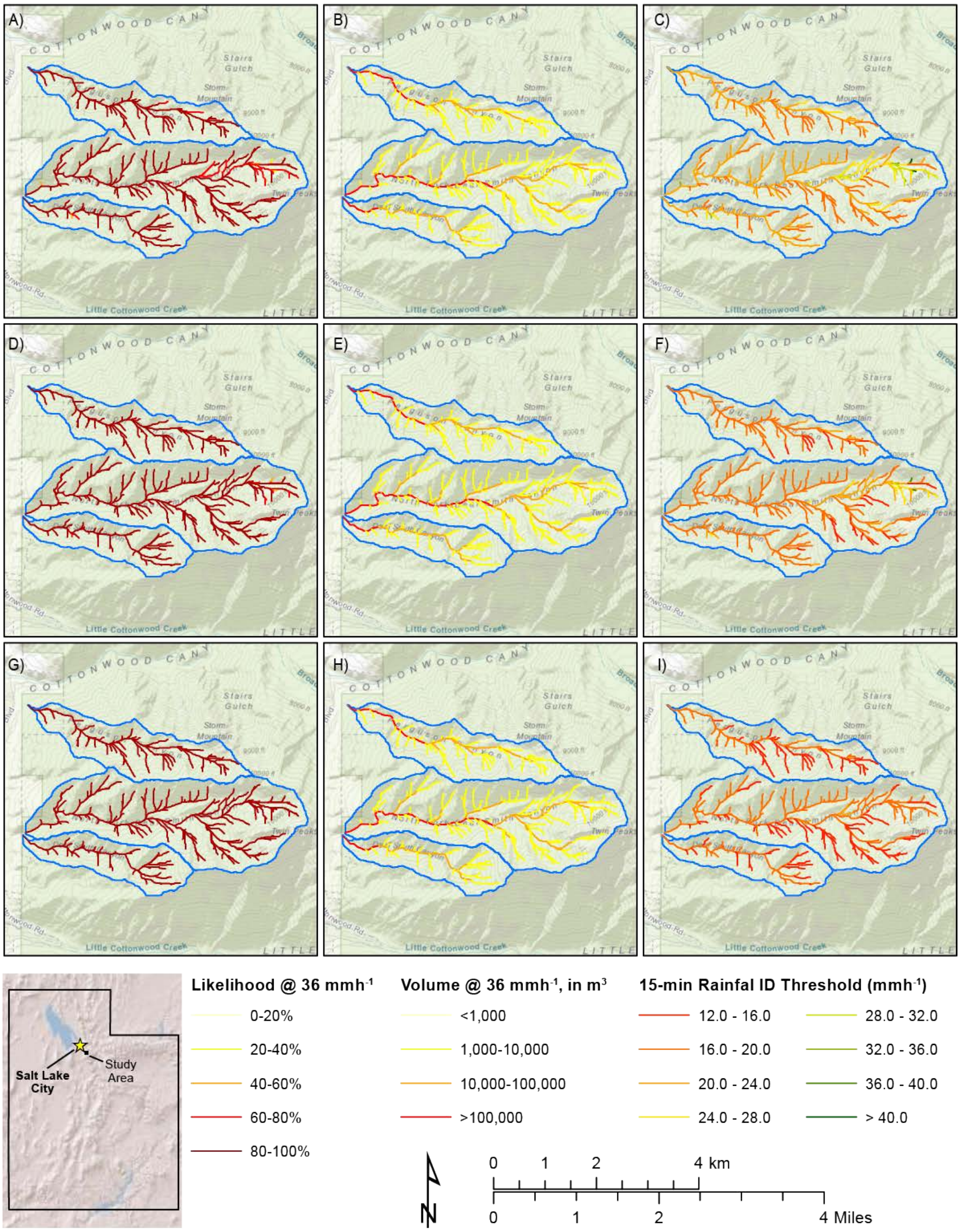

Fig. S6. Simulation results for three canyon above suburban Salt Lake City at three fire severity scenarios: P_{dsim} = 0.5 (A, B, and C), P_{dsim} = 0.75 (D, E, and F), and P_{dsim} = 0.9 (G, H, and I). The three canyons from north to south, are Ferguson Canyon, North Fork Deaf Smith Canyon, and Deaf Smith Canyon. Simulated likelihood (H_L) for a storm with a peak 15-minute intensity of 36 mmh^{-1} (A, D, and G), simulated volume (H_V), in m^3, for a storm with a peak 15-minute intensity of 36 mmh^{-1} (B, E, and H), and simulated 15-minute rainfall intensity-duration threshold (H_{T15}), in mmh^{-1} (C, F, and I).